PARAMETRIC DESIGN AND DIGITAL FABRICATION OF CURVED ORIGAMI STRUCTURES REALIZED BY TWISTING ACTIVE PANELS

Ilaria Giannetti
Alessia Bisconti
Alessandro Tiero
Andrea Micheletti

Curved origami surfaces attract significant attention in architecture and engineering for the design of form-resistant modular structures. The realization of curved origami surfaces requires suitable structural design tools, manufacturing techniques, and construction methods. Here, a design workflow for the realization of curved origami structures assembled from flexible panels is proposed. Each flexible panel is realized as an interconnected array of beams according to the notable lamina-emergent torsion motif, with the result that panel bending is linked to the twisting of the beams. An analytical mechanical model for the bending of panels into cylindrical surfaces is described first. Then, such model is adapted to conical surfaces. This model is instrumental in determining the maximum achievable curvature of a cylindrical or conical flexible panel, and the corresponding stresses, as a function of the geometric features of the lamina-emergent torsion motif and of the material properties. The design workflow has two phases, the geometry design, in which a folded curved-origami geometry with corresponding crease pattern and surface ruling are chosen, and the design of the geometric features of the flexible panels. A parametric digital model was implemented using commercial software to carry out both phases, and two different literature computer codes were employed to simulate the origami folding process. The design workflow was demonstrated by the realization of physical prototypes using the laser cutting technology, and it can be applied at different scales to the manufacturing of curved origami structures. The case of an outdoor installation demonstrates the potential of the proposed design workflow for architectural structures.

INTRODUCTION

Since the 20th century, curved surfaces attracted significant attention in architecture and engineering for the design of form-resistant structures [1]; more recently, origami-inspired structures [2] and curved origami modular structures were also developed. The complex forms of curved origami surfaces require appropriate design methods and advanced tools for their realization as architectural and engineering structures. Several studies have been dedicated to the analytical geometric design of such surfaces. For example, an optimization procedure was proposed for the design and digital reconstruction of surfaces obtained by curved folding [3], and, a rationalized curved folding was presented to design origami mechanisms with one degree of freedom [4]. Moreover, a geometric mechanics model was described to study the folding behavior of curved origami [5], and, multilayered surfaces were assembled from rigid-foldable curved origami structures [6]. Furthermore, curved origami with multiple states were studied [7], a discrete elastic model was formulated for the structural analysis of curved origami [8], and systematic design methods for curved origami were presented [9]. At present, research on effective construction techniques for curved origami is still in an exploratory phase, and only a few literature studies have presented actual realizations

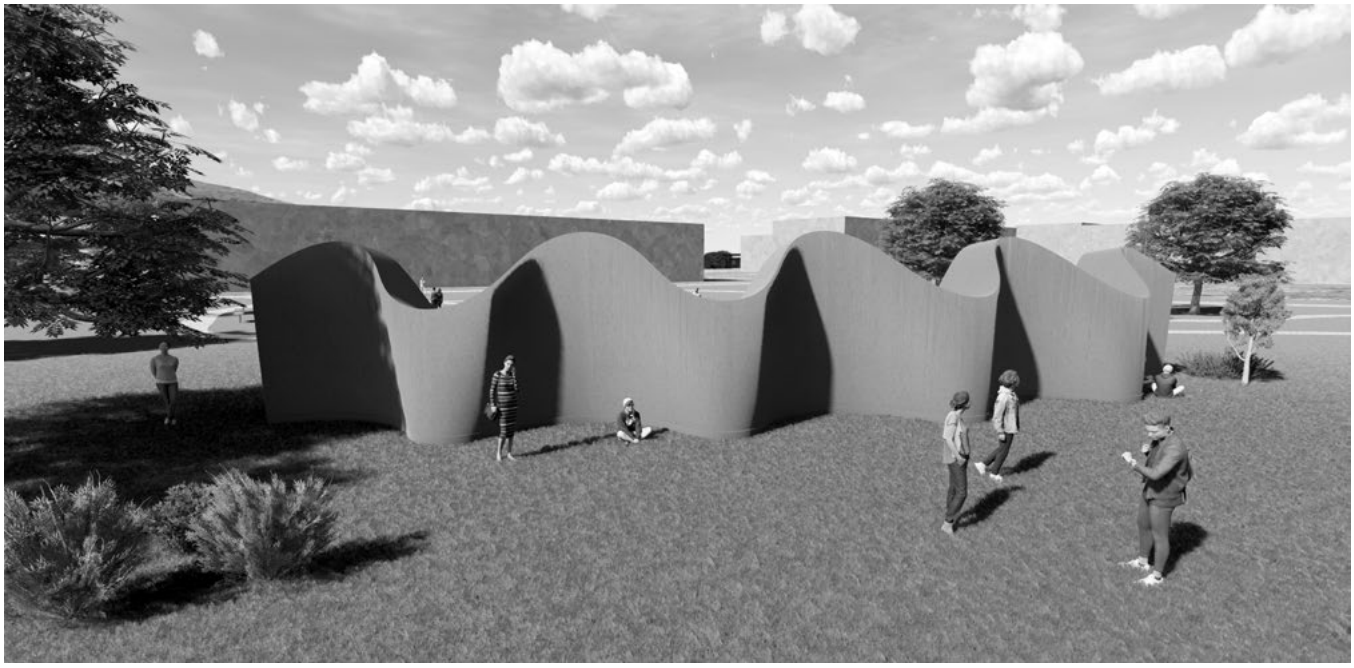

Figure 1: Computer view of an outdoor installation based on a curved origami surface.

or practical design solutions. For instance, the design and realization of two meter-scale prototypes folded and assembled from aluminum thin sheets were analyzed [10], a class of curved crease patterns were employed to create spatial structural enclosures composed of cylindrical and conical surfaces [11], and, accordion-like mechanisms obtained from flat plates with curved creases were designed to obtain corrugated spatial structures [12]. Here, a design workflow for the realization of curved origami structures assembled from flexible twisting-active panels is presented. Each panel is realized as a perforated plate according to the notable lamina-emergent torsion motif [13], in which an interconnected array of beams is subjected to torsion when the panel flexes. Lamina-emergent arrays were proposed to facilitate deployable mechanisms based on curved origami [14], and to assemble double curvature surfaces [15]. In addition, a lamina-emergent flexural connection was proposed [16], while laminar arrays were evaluated for the realization of compliant hinges for thick origami structures [17]. The presented methodology focuses on the use of an analytical mechanical model integrated with parametric modeling and physical prototypes. The mechanical model aims to determine the maximum curvature of the panels under cylindrical and conical bending, depending on the geometric features of the perforation pattern and the mechanical properties of the material. This model is then integrated with a parametric design tool with the aim of optimizing and automating the manufacturing process. Such approach has enabled the production of prototypes in various materials, particularly MDF (medium density fiberboard) and PMMA (polymethyl methacrylate), which have been analyzed to assess the impact of the perforation pattern on flexibility and strength. The use of the parametric and algorithmic simulation tool Grasshopper™ has allowed for a refined manipulation of the design variables and greater optimization of the final product. The proposed design workflow has two phases. The first phase consists of the design of the folded curved-origami geometry and of the corresponding surface ruling and crease pattern. In the second phase, the origami surface is subdivided into several panels, each with a perforation pattern whose geometric features are derived from the surface ruling and curvature. The design case of an outdoor installation, depicted in Figure 1, illustrates in detail the steps of the workflow. The paper is structured in two main sections: the first section presents the analytical mechanical model for the design of the twisting active panels, considering both the cylindrical and the conical surfaces; the second section presents the subsequent steps of the adopted design workflow referring to the case of an outdoor installation.

TWISTING ACTIVE PANELS

In this section, the analytical mechanical model of the twisting active panel is presented referring to cylindrical and conical bending, respectively. In both cases, the panels feature lamina-emergent torsion arrays aligned with the ruling of the surfaces. The model is instrumental in determining the maximum achievable curvature of the flexible panels and the corresponding stresses, as a function of the geometric features of the lamina-emergent torsion (LET) motif and of the material properties.

Cylindrical bending

For the analysis of the flexible panel for cylindrical surfaces, we adopt a modified version of the model presented by Oshima et. al [18]. A flexible panel is considered as an assembly of rigid blocks and linearly elastic beams, in which all beams undergo a twisting deformation when the panel is deformed into a cylindrical shape. Figures 2 (a) and (b) show a view of a bent panel and a detail of the LET motif, where we distinguish solid parts (beams and rigid blocks) and perforated parts. With reference to Figures 2 (c) and (d), the following parameters are identified. Each beam has width *t*, height *h*, and length *l*. The width of each rigid blocks is 2*d* and each perforated hole has width *s* and length 2(l+*d*). The distance between the axis of adjacent beams is *a*, while the distance between rigid blocks is *b*. The number of beams counted along the x-axis (y-axis) is 2*n* (*m*).

Two equal and opposite external couples of magnitude C are applied to the solid edges parallel to the beams' axis, as shown in Figure 2 (c) and (d). We assume that, in bending the panel in the $x - y$ plane, all beams are subjected to the same twisting moment M_T. Given that each rigid block carries the twisting moments of two beams (Figure 2 (e)), and that the panel can be split in two parts by sectioning *n* rigid blocks along the x-direction, the following equilibrium condition holds:

(1) $$C = 2M_T n\,.$$

The torsion stiffness s_T is given by:

(2) $$s_T = G\,J_T\,,$$

where G is the shear modulus of the material and J_T is the torsion constant of the rectangular cross section of the beam, expressed by ($h > t$)

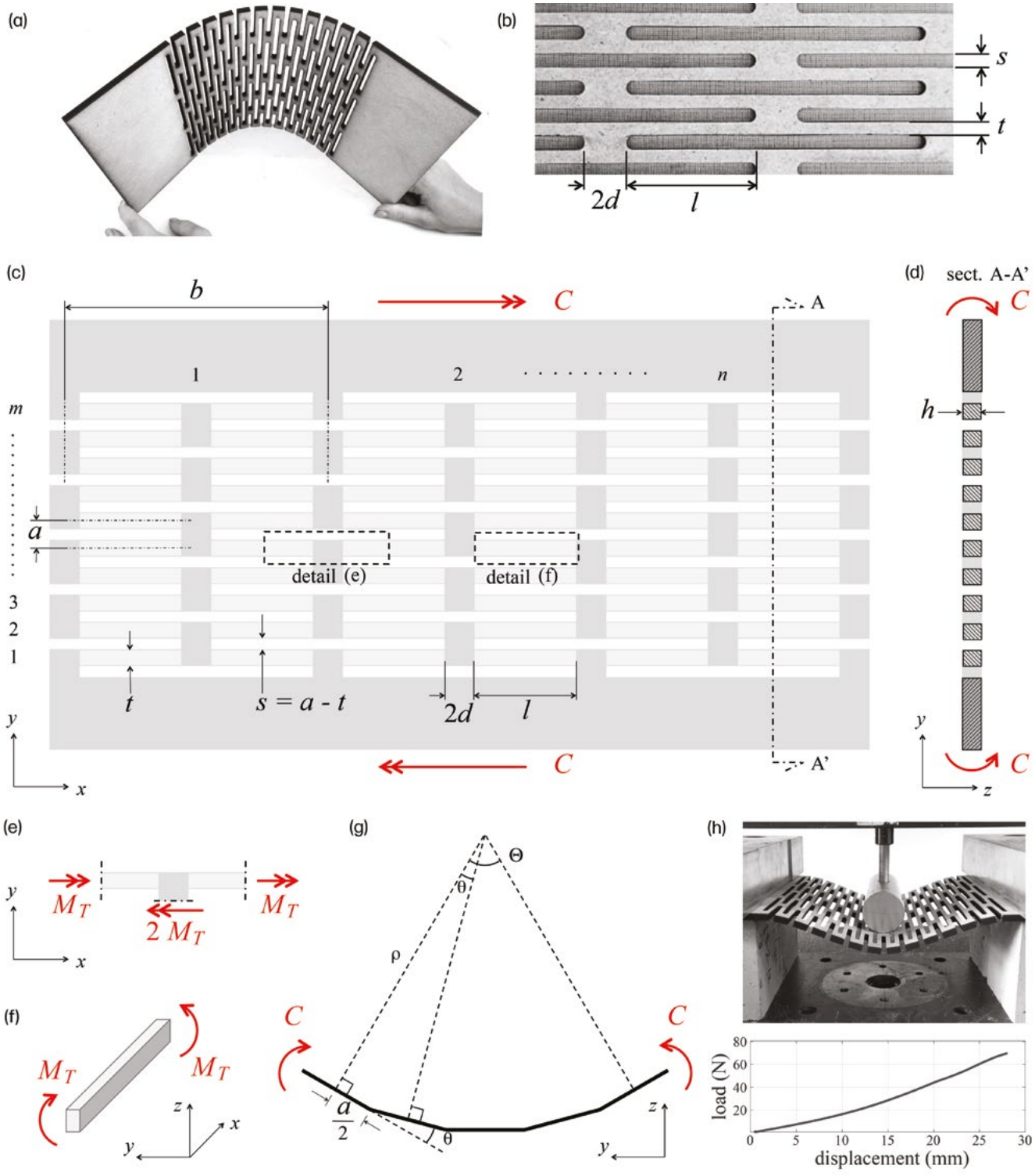

Figure 2: Cylyndrical bending model. (a) View of the flexible panel subjected to testing. (b) Detail of the LET motif. (c-f) Plan view, cross section, and details of the model. (g) Representative deformed configuration. (h) Sample subjected to flexural test and load vs. displacement curve. Conical bending.

(3)

$$J_T = \frac{1}{16} h t^3 \left(\frac{16}{3} - 3.36 \frac{t}{h} \left(1 - \frac{t^4}{12 h^4} \right) \right) .$$

The twisting angle, θ, associated to the twisting moment M_T, is calculated as:

(4)

$$\theta = \frac{M_T}{s_T} l .$$

This angle is also equal to the relative rotation between the rigid blocks of adjacent sections of the flexible panel, as shown in Figure 2 (g).

The action of the couples C that bend the panel induces the total relative rotation angle Θ between the two end sections, which can be computed as the summation of the relative rotation angles between adjacent sections.

We have:

(5)

$$\Theta = m\theta = m \frac{M_T}{s_T} l = \frac{1}{2} \frac{m}{n} \frac{C}{s_T} l .$$

A discrete curvature radius ρ, related to the twisting angle θ, can be obtained from the relation (cf Fig. 2, g)

(6)

$$\rho \tan\left(\frac{\theta}{2}\right) = \frac{a}{2} .$$

When θ is small, we can consider that tanθ ≈ θ and define the curvature κ as:

(7)

$$\kappa = \frac{1}{\rho} = \frac{\theta}{a} .$$

With this relation, using (1) and (4), the bending couple can be expressed as:

(8)

$$C = 2 n s_T \frac{\theta}{l} = 2 n s_T \frac{a}{l} \kappa .$$

Finally, the couple per unit width of the panel, 2, is calculated as

(9)

$$c = \frac{C}{nb} = 2 \frac{a}{b} \frac{s_T}{l} \kappa = \tilde{s}_B \kappa ,$$

In the last equality in (9), $\tilde{s}_B$ is the equivalent plate bending stiffness:

(10)

$$\tilde{s}_B = 2 \frac{a}{b} \frac{s_T}{l} .$$

These relations lay the foundation for understanding the behavior of LET panels when subjected to cylindrical bending. The correlation between the material's mechanical properties, the geometric dimensions of the panel, and the applied forces allow us to predict the panel's response in terms of curvature and twisting moment. The torsion verification of the rectangular cross section of the beams, according to standard regulations, allows the evaluation of the maximum radius of curvature ρ that the panel can achieve, which is fundamental to guarantee its structural integrity under load, ensuring that it can withstand expected stresses without incurring damage or permanent deformation. In particular, the maximum design shear stress for torsion is:

(11)

$$\tau_{tor,d} = k_{sh} f_{v,d} ,$$

where $k_{sh} = 1 + 0.15\, h/t$ is a coefficient taking into account the shape of the cross-section and $f_{v,d}$ is the design shear strength. The maximum shear stress for rectangular sections can be computed as:

(12)

$$\tau_{tor,d} = \alpha \frac{3 M_T}{t^2 h} ,$$

with α expressed by:

(13)

$$\alpha = 1 + 0.6095 \frac{t}{h} + 0.8865 \left(\frac{t}{h}\right)^2 - 1.8023 \left(\frac{t}{h}\right)^3 + 0.9100 \left(\frac{t}{h}\right)^4 .$$

By combining (4), (7), and (12), the design maximum curvature is obtained:

(14)

$$\kappa_d = \frac{t^2 h}{\alpha} \frac{k_{sh} f_{v,d}}{s_T} \frac{l}{a} .$$

A flexural test was conducted in the Laboratory of Structures, Tests, and Materials of the University of Rome Tor Vergata to evaluate the mechanical properties of the prototypes created. A sample in MDF with dimensions 400x220x6 mm (Figure 2 (a)) was prepared, which included solid parts at the edges to be clamped in the testing machine. The geometric parameters chosen for the LET motif for the sample are reported in Table 1 (cf. Figure 2). The sample was subjected to a gradually increasing displacement in the center until a displacement of 30 mm was reached (Figure 2 (h)), with a speed of the testing crosshead of 5 mm/min.

n	*m*	*a*	*b*	*h*	*t*	*l*	*d*
3	26	8mm	70mm	6mm	4mm	25mm	5mm

Table 1. Geometric parameters of the tested sample.

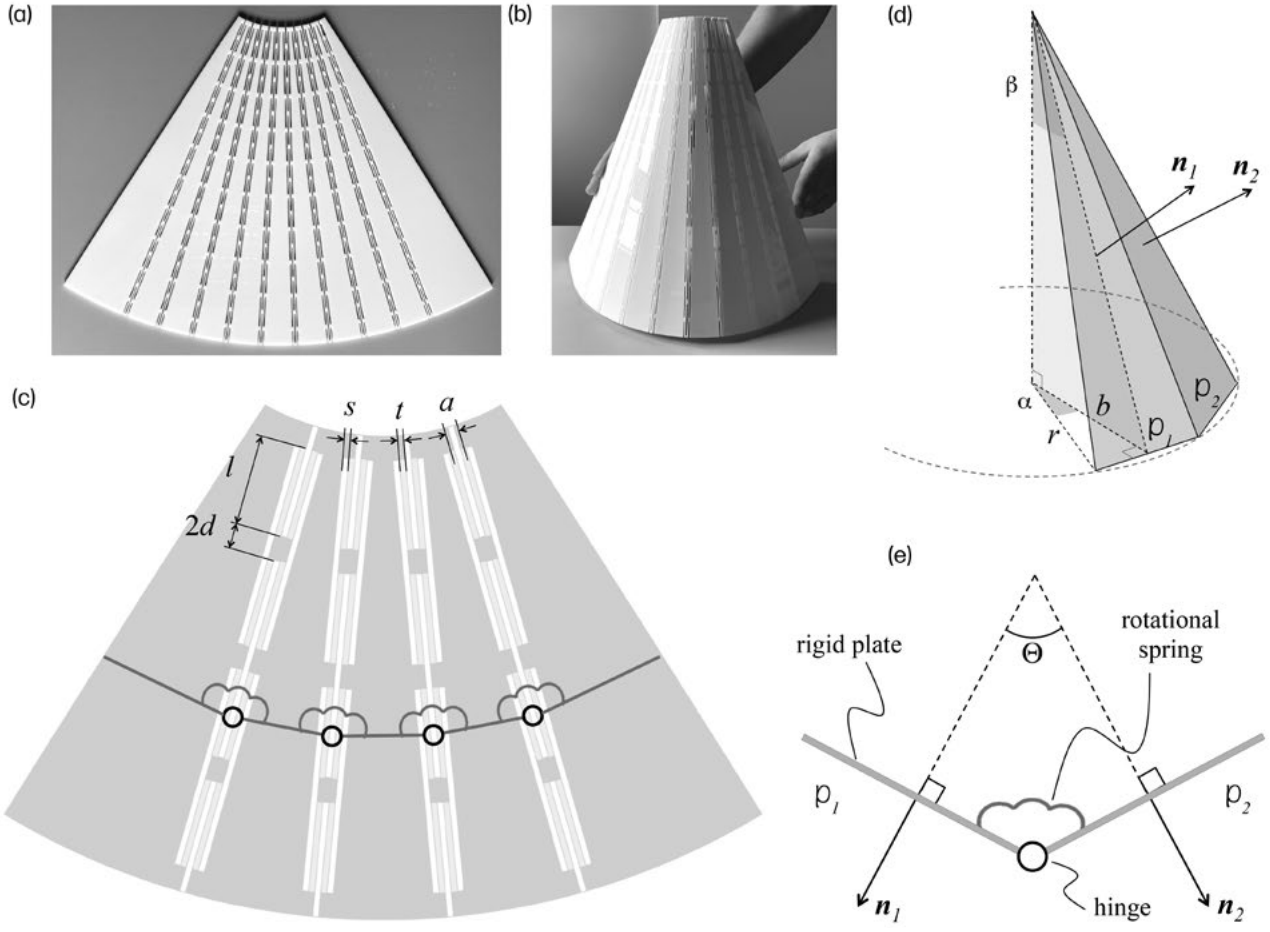

Figure 3: Adaptation of the LET motif to conical bending. (a,b) fabricated desktop prototype. (c) Schematization in rigid plates connected to each other by compliant hinges, realized by LET connections and modeled as rotational springs. (d) Deformed shape of two adjacent plates, geometric parameters and normal vectors. (e) Two adjacent panels connected by a compliant hinge sectioned by a plane containing the normals.

Geometry design

i: Choice of the curved-crease pattern

ii: Choice of the ruling

iii: Definition of the design parameters

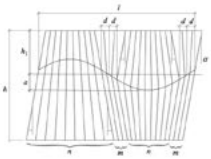

iv: Rigid-folding kinematics

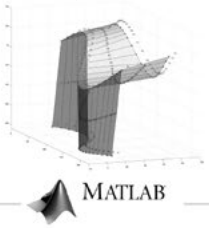

Flexible panel design

v: Parametric study of the LET motif

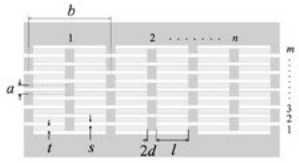

vi: Prototypes production

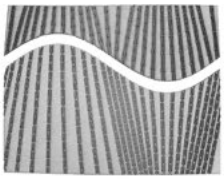

vii: Construction details

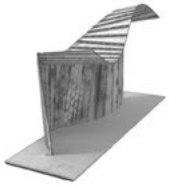

Figure 4: Design and production steps.

Series of arcs

Sinusoid

Series of arcs and lines

Series of semicircles

Polyline

Figure 5: Typological studies of the curved crease (in red the chosen curve).

Symmetrical cones combination

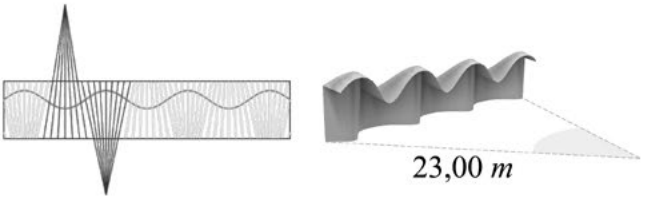

Non-symmetrical cones combination

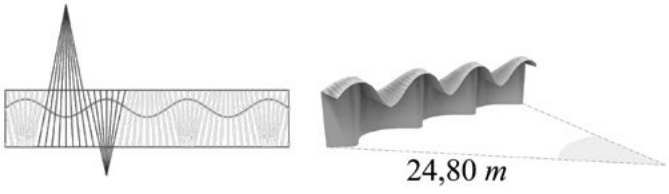

Cones and cylinders combination: version 1

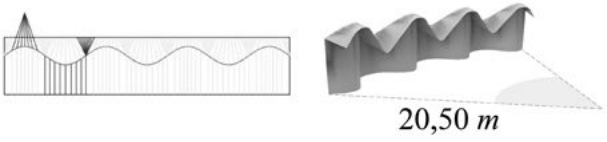

Cones and cylinders combination: version 2

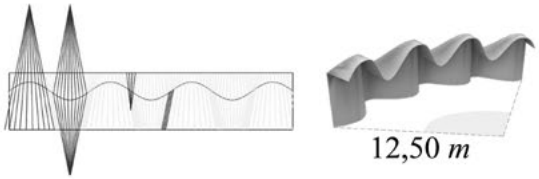

Figure 6: Study of the ruled surface pattern (in red the chosen pattern).

At the beginning of the test, under a small imposed displacement, the deformation of the sample is comparable to that of a clamped-clamped beam loaded in the center, showing a predominant bending behavior and linear response. As the imposed displacement increased, the panel began to stretch in-plane, and a nonlinear stiffening effect was observed from the force vs. displacement curve. The initial stiffness was calculated from the data of the flexural test and compared with that obtained analytically. The stiffness calculated using two test data points near the origin, (δ_1, f_1), (δ_2, f_2), is $k_{test} = (f_2 - f_1)/(\delta_2 - \delta_1) = 1.484\ ^{10-3}$ kN/mm. The analytical calculation considered the stiffness constant for the transverse displacement at the midpoint of a clamped-clamped Euler-Bernoulli beam, given by $k_{an} = 192\, s_B/l^3_B$, with $s_B = nb\, \check{s}_B$ (cf. (9)) and $l_B = ma$. By considering the value G = 800MPa for the shear modulus of the MDF, the calculated stiffness is $k_{an} = 2.174\ ^{10-3}$ kN/mm. This value is higher than that measured in the test, as it should be, reflecting the fact that the deformation of the portions of the panel corresponding to the rigid blocks in the model is neglected.

Conical bending

In the conical case, the rows of perforations are placed along the generatrices, leaving large unperforated trapezoidal areas that act as rigid plates (Figure 3 (a,b)). The panel is considered an assembly of rigid plates connected to each other by compliant hinges realized by LET connections and modeled as rotational springs (Figure 3 (c)). The rotational stiffness of such springs can be computed from (8) in terms of the parameters that define the LET connection. The deformed configuration of two adjacent rigid plates can be described by the parameters depicted in Figure 3 (c,d): *a, β, r, b*, and Θ. The angle Θ formed by the normal vectors $\mathbf{n}_1$ and $\mathbf{n}_2$ of two adjacent panels can be calculated in terms of *α* and *β* from the following expression,

(15)
$$\cos\Theta = \frac{\mathbf{n}_1 \cdot \mathbf{n}_2}{\|\mathbf{n}_1\|\|\mathbf{n}_2\|} = (\cos\beta)^2 \cos(2\alpha) + (\sin\beta)^2 .$$

Using a Grasshopper™ code it was obtained a parametric LET perforation pattern featuring rectangular holes with rounded corners. The slits pattern follows the ruling of the conical surface. The desktop prototype shown in Figure 3(a,b) was produced with the laser cutting machine on a Perspex panel of 300x400x3 mm, and it is characterized by 10 lamina-emergent arrays, each with three rows of 1mm slits, spaced 1.5mm apart and 2.5 cm long.

Design application

This section focuses on the design of a curved origami outdoor installation composed of flexible twisting-active panels. The design process exploits parametric design tool Grasshopper™, Origami Simulator [19], and MATLAB codes.

The design workflow, shown in Figure 4, articulates in two main phases: the study of the geometry of the curved origami (Steps i-iv) and the design of flexible twisting-active panels (Steps v-vii), exploiting both cylindrical and conical surfaces (Figure 4).

The geometry of the outdoor installation is modular. The base module refers to a curved origami composed of a single wavy mountain fold on a rectangular shape. The repetition of the base module suggests the study of a sine wave-like curve contained in an oblong rectangle. The subsequent definition of the folded configuration comprises the parametric study of the sine wave-like curve and of the related ruling surface. The design of the flexible panels follows the definition of the ruling and develops through the study of the LET slit pattern.

Geometry design

The study of geometry is organized in four steps and is described below. The combined use of the Grasshopper™ code and Origami Simulator supports steps i and ii, i.e., the parametric study of the crease pattern and the simulation of the fold. Steps iii and iv require the use of GrasshopperTM and a MATLAB code to simulate the kinematics of the rigid folding.

i. *Typological studies of the curved-crease pattern*: The geometry of the mountain fold curve is defined by comparing a series of arches, a series of arches and lines, a series of semicircles, a polyline and a sinusoid (Figure 5). A Grasshopper™ code is used for the parametric analyses of each curve and for the definition of the related ruling surface. A simulation of the fold is, thus, conduced, exploiting Origami Simulator, for each of the five crease patterns. Result of the simulation shows the sinusoid as the best option for the mountain fold.

ii. *Study of the ruling surface pattern*: The definition of the design ruling is conducted combing portions of cylindrical and conical surfaces. The study follows an iterative process based on the combined use of a Grasshopper™ code, for the parametric definition of the mountain fold curve and the ruling pattern, and Origami Simulator for the simulation of the fold. As shown in Figure 6, four combinations of cylindrical and conical surface are considered: a symmetrical combination of conical surfaces; a non-symmetrical combination of conical surfaces; the combination of two types of conical surfaces and one type of cylindrical surface; the combination of three types of conical surface and a band-like cylindrical surface.

The four considered combinations are compared through the simulation of the fold: as shown in Figure 6, the folded structures, related to the four combinations of conical and cylindrical surfaces, are inscribed respectively in a 23.00 m-radius circle, in a 24.80 m-radius circle, in a 20.50 m-radius circle, and in a 12.50 m-radius circle. Result shows, thus, the latter configuration as the most effective in terms of folding capabilities.

iii. *Definition of design parameters*: For the sinusoid the considered geometrical parameters are the amplitude A and the period L. The other relevant design parameters for the panel dimensions and the surface ruling are illustrated in Figure 7. According to the architectural functionality of the structure, the period L was taken equal to 6.30m while the wave amplitude A is equal to 0.70 m. In the dimensional assessment, the balance between the elevation and the cantilever span of the structure is considered: according to the defined value of the sine wave amplitude, the cantilever span range from $H_1 - A$ = 0.85m to $H_1 + A$ = 2.25 m; the minimum value of the structure elevation was set as $H - (H_1 + A)$ = 2.30m and, consequently, the maximum value of the pavilion elevation is $H - (H_1 - A)$ = 3.70 m. The ruling of the conical and cylindrical surfaces is defined respectively by the parameters *N* and *M* that indicates the number of subdivisions. The parameter D determines the width of the cylindrical surface, and it is equal to 0.50 m. The angle α corresponds to the inclination of the ruling and it is equal to 11 degrees.

iv. *Rigid-folding kinematics:* Given that the underlying mechanical model in Origami Simulator accounts for the out-of-plane elastic deformation of the tiles, the accuracy of the folding process and of the folded geometry was verified by adopting the rigid-origami MATLAB™ calculation platform introduced and detailed by Micheletti et al. [20, 21]. The interoperability of Grasshopper™ and MATLAB™ was exploited to export the origami data from Grasshopper™ and import it into the MATLAB™ code. The crease pattern of the rigid origami was obtained by segmenting the sinusoidal crease and by considering the subdivisions of the ruled surfaces as shown in Figure 7. Such rigid origami has one degree of freedom. The folding process was simulated numerically by imposing the folding angle at the curved crease. The output geometry of the rigid folding process is depicted in Figure 8.

Flexible panel design

The design of flexible panels develops through the study of the LET arrays. It consists of three steps supported by the use of Grasshopper™ and laser cutting technology to produce physical prototypes. The three steps are described below.

v. *Parametric study of the LET pattern*: A Grasshopper™ code is developed for the parametric study of the LET motif and the production of prototypes exploiting laser cutting. The code allow to assess the following parameters: *N* and *M*, as the numbers of subdivisions of the conical and cylindrical surfaces respectively (Figure 7); *l* as the length of the beams, *t* as the width of the beam; *s* as the width of the slits; 2*d* as the width of the rigid blocks; *a* as the interaxis between the beams, and *b* as the interaxis between the rigid blocks (Figure 2). The geometrical construction of the LET pattern develops through the offset of the curves composing the ruling, controlled by the *s* and the *t* values, and the subsequent subdivision of the same curves according to the value of the *l* and *d* parameters. The code comprises, eventually, the possibility to control the fillet of the slits corners, which is necessary to avoid stress concentration effects.

The base module of the designed structure corresponds to the period of the wave curve and is composed of four panels. As shown in Figure 9, to obtain the four panel the base module is divided vertically and horizontally. The vertical subdivision corresponds to the end of the conical surface and the start of the cylindrical band. The horizontal subdivision corresponds to the mountain fold curve: the lower part forms the wall-panel while the upper part the cantilever-panel of the designed structure. Dimensions and geometry of the four panels are reported in Figure 9. The first wall-panel *is a conical surface:* the value of the *N* parameter (number of subdivisions) is equal to 35. The second wall-panel is composed of two side sectors of cylindrical surfaces – for both sides the value of the *M* parameter (number of subdivisions) is equal to 9 – and a central sector of conical surface – with the same value of *M*. The first cantilever panel is a conical surface while the second cantilever panel is composed of two side-sector of cylindrical surfaces and a central sector of conical surface, with corresponding values of *N* and *M*. For all panels, the value of the *l* parameter (length of the beams of the LET motif) is equal to 88mm and the values of the C parameter (width of the beam) and the *t* parameter (width of the slits) are both equal to 4 mm; the *d* parameter (half-width of the rigid blocks) is equal to 6 mm.

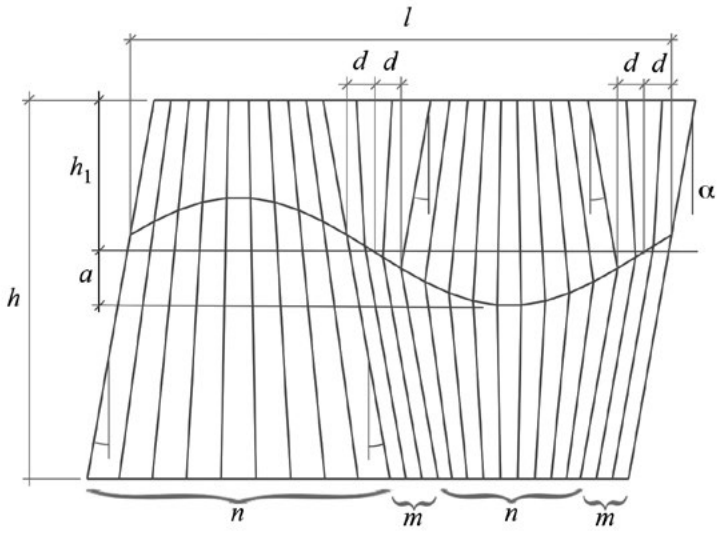

Figure 6: Study of the ruled surface pattern (in red the boundaries between conical/cylindrical rulings).

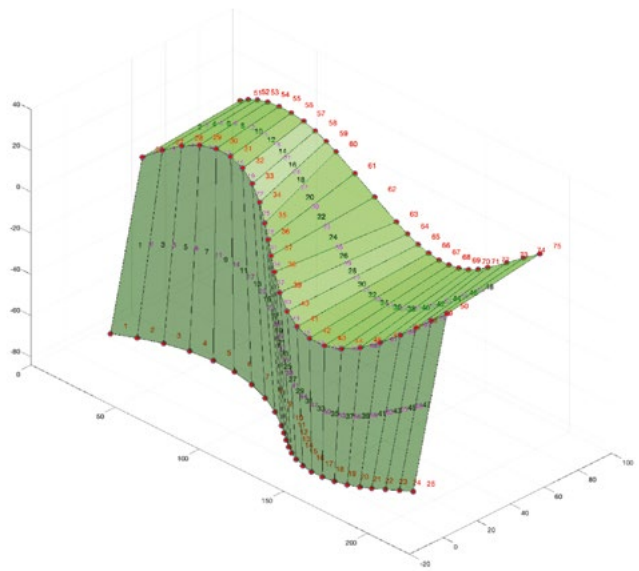

Figure 8: Rigidly folded configuration of a representative module simulated in the MATLAB™ calculation platform described Micheletti et al. [20, 21].

a)

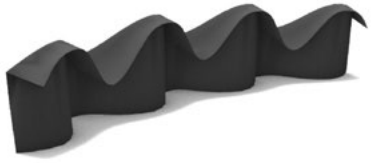

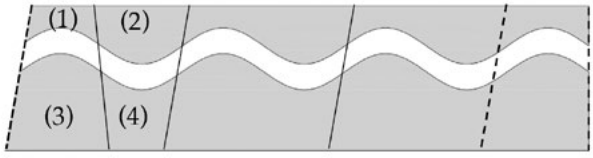

b)

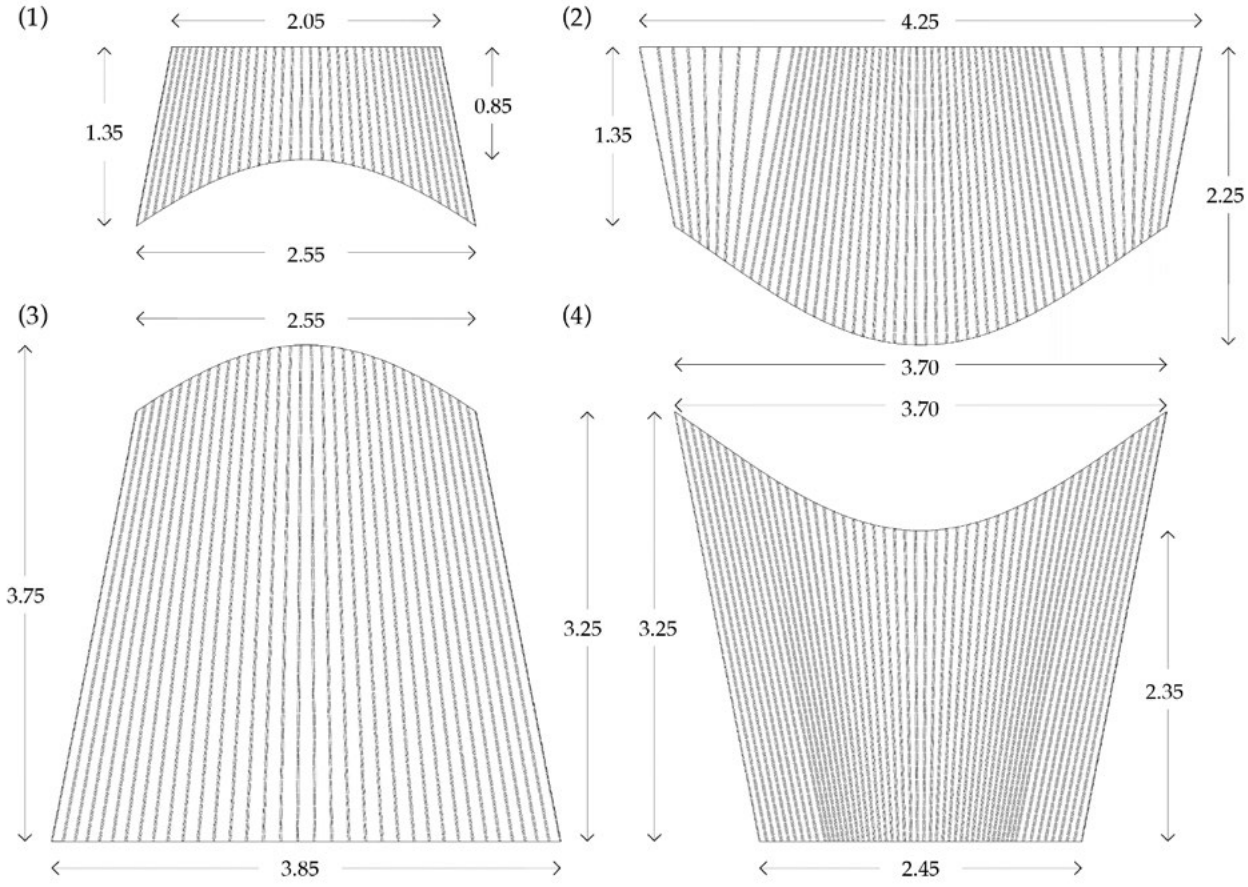

Figure 9: The four base panels of the structure. Dimensions are expressed in meters.

vi. *Prototype production:* An appendix of the Grasshopper™ code was developed to produce the 1:10-prototype of the designed structure, taking advantage of laser cutting technology and FDM desktop 3D printing. The material choose for the laser cut prototype is a 4 mm thick MDF panel. The prototype is composed of two panels. As shown in Figure 10, the two panels are obtained subdividing a rectangular module – 0,46 m height and 0,62 m wide – of the designed structure on the mountain fold curve: the lower part forms the wall panel while the upper part the cantilever panel. Both the wall and the cantilever panels are composed of two conical side portions and central cylindrical band. For the adopted slits pattern the value of the *l* parameter (length of the beams of the LET motif) is equal to 19mm and the values of the *t* parameter (width of the beam) and the *s* parameters (width of the slits) are both equal to 2 mm; the *d* parameter (half-width of the rigid blocks) is equal to 3 mm. To assure the folding of the structure, the horizontal connections between the wall and the cantilever panels is composed of a set of steel hinges located on the mountain fold and fixed on the panels by bolts. The Grasshopper™ code was implemented to produce a further small-scale prototype exploiting the FDM desktop 3D printing technology. This small scale prototype, shown in Figure 12 aims to explore further alternative of the joints between the wall and the cantilever panels, avoiding steel connections and exploiting tensile bands.

vii. *Construction details:* The production of the prototypes supports the study of construction details of the designed structures. The study focuses, in particular, the connections composed of reversible devices in order to assure the disassembly and the re-usability of the designed structure. A reversible dry joint is designed for the vertical connection between the four panel, exploiting a C-shape-element fitted into the slit of the LET motif at the ends *of the panel.* The C-shape element can be produced exploiting laser cutting – as it is in the presented prototype – or can be substituted by a standard profile in steel. To assure the folding of the structure, the horizontal connections between the wall and the cantilever panels is composed of steel hinges located on the mountain fold and fixed on the panel by bolts. The connection to the grounds are also designed exploiting commercial steel plates – functioning as basement – fixed removable bolts. A possible alternative to the hinge joints between the wall and the cantilever panels is represented by the use of tensile bands as a stitching within the two elements.

CONCLUDING REMARKS

In this study, the design of curved origami structures assembled from twisting active panels was performed, with a particular focus on the analytical and experimental characterization. The exploration included the development of LET patterns for ruled cylindrical and conical surfaces and the study of the interaction between ruled and folded geometries. The adoption of a methodological approach that combines an analytical model with parametric modeling tools facilitates the production of physical prototypes, exploiting digital fabrication technologies, in order to assess the folded configuration and the building details of the origami structure. The investigations revealed the effectiveness of the proposed methodological approach in analyzing the curvature and in the sizing of the twisting-active panels, which feature a pattern of perforations, intended for ruled surfaces, in both cylindrical and conical configurations. Parametric modeling has proven to be a reliable mean for rapid prototyping and has provided indispensable visual support in the architectural design process. Moreover, the use of laser cutting as a production methodology of the prototype has favorably contrasted with conventional methods, such as 3D milling, in terms of time and cost of the process. In this sense, the study envisaged also the production of the prototypes with 3D printing techniques, exploiting the already produced Grasshopper™. From a structural design perspective, the study introduced a scalable design and realization method for lightweight modular structures, adaptable to various application fields, including interior design, construction, morphological structures, and robotics [22,23]. Particular application examples in the building sector are: centering systems for modular reiforced concrete shells based on ruled surfaces, lightweigth structures for curved façades, and acoustic barriers for open spaces. The dimensions of the modules are chosen so as to satisfy the size of the laser cutting machine, supporting the design of elements of reduced size easy to transport and to assemble without the need of heavy machinery. The proposed analytical approach permits the fast selection of the thickness and curvature of the elements to fulfill the structural requirements, supporting customized production based on digital fabrication. However, several important challenges remain, particularly the development of a mechanical model for conical and tangential developable surfaces in relation to various cutting patterns. This area requires additional research to further refine the design and address the remaining technical challenges by advancing the field of state-of-the-art structural design.

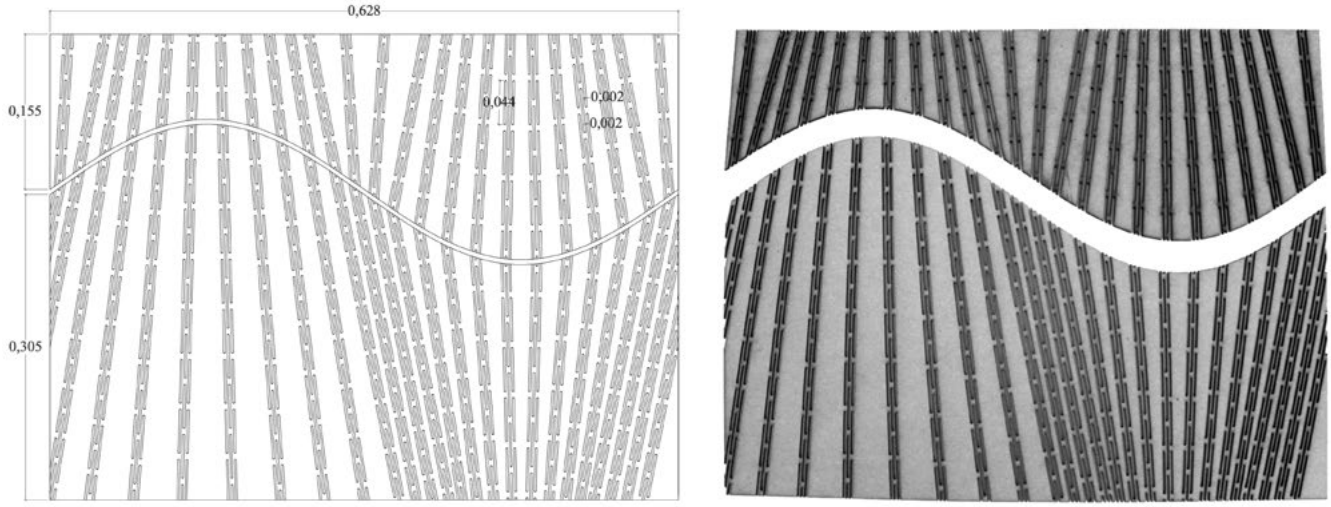

Figure 10: Prototypes panels (scale 1:10).

Figure 11: Laser cut prototype (scale 1:10) connected with hinges to reproduce a module of the outdoor installation.

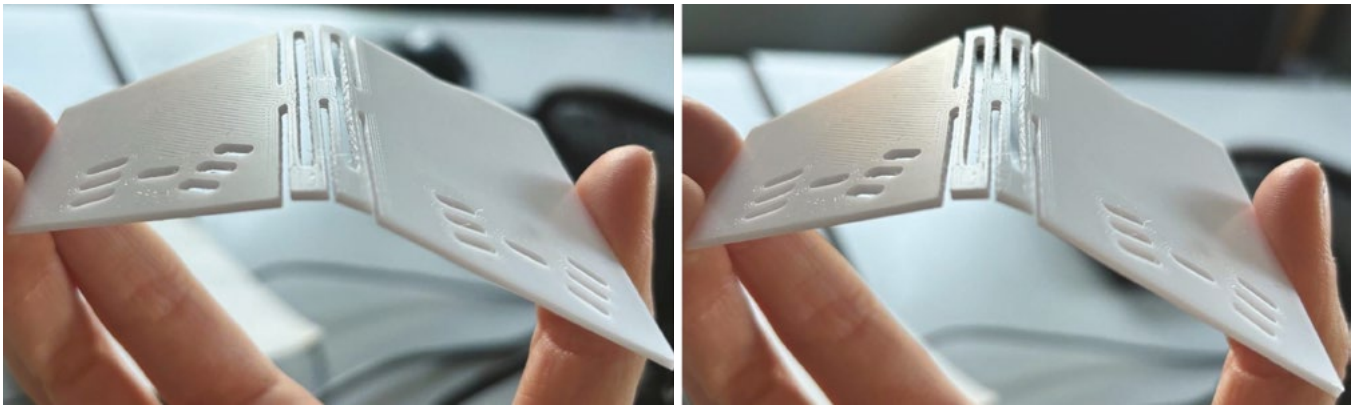

Figure 12: 3D printed small scale prototype.

ACKNOWLEDGEMENTS

The authors thank Claudio Intrigila for the assistance he provided during the experimental testing of flexible panels. The contribution received from Alessia Terrezza, Valeria Magnani, and Giulia Sergi for the realization of physical prototypes is gratefully acknowledged.

REFERENCES

[1] S. Anderson (Ed.), Eladio Dieste Innovation in Structural Art, Princeton Architectural Press, New York 2004.

[2] C. Robeller, Y. Weinand, Interlocking Folded Plate – Integral Mechanical Attachment for Structural Wood Panels. International Journal of Space Structures, 30(2), pp. 111-122, 2015. doi: 10.1260/0266-3511.30.2.111

[3] M. Kilian, S. Flöry, Z. Chen, N. Mitra, A. Sheffer, H. Pottmann, Curved folding, ACM Trans. Graph. 27 (08), 2008. doi:10.1145 /1399504.1360674.

[4] T. Tachi, G. Epps, Designing one-dof mechanisms for architecture by rationalizing curved folding, in: Proceedings of the Int. Symposium on Algorithmic Design for Architecture and Urban Design, ALGODE TOKYO 2011, 2011.

[5] M. A. M. Dias, L. Dudte, L. Mahadevan, C. Santangelo, Geometric mechanics of curved crease origami, Physical Review Letters 109 (06 2012). doi: 10.1103/PhysRevLett.109.114301., 1997.

[6] T. Tachi, Composite rigid-foldable curved origami structure, in: Proceedings of the 1st Conference Transformables 2013, 2013.

[7] T.-U. Lee, Y. Chen, J. Gattas, Curved-Crease Origami with Multiple States, in: Origami 7: 7th Int. Meeting of Origami Science, Mathematics, and Education, pp. 849–864, CRC Press, 2018.

[8] S. R. Woodruff, E. T. Filipov, A bar and hinge model formulation for structural analysis of curved-crease origami, International Journal of Solids and Structures, 204-205, pp. 114–127, 2020. doi:10.1016/j.ijsolstr.2020. 08.010.

[9] H. Liu, R. D. James, Design of origami structures with curved tiles between the creases, Journal of the Mechanics and Physics of Solids, 185, 105559, 2024. doi: 10.1016/j.jmps.2024.105559.

[10] P. Eversmann, P. Ehret, A. Ihde, Curved-folding of thin aluminium plates: towards structural multi-panel shells, in: G. M. Bögle, A. and (Ed.), Proceedings of the IASS Annual Symposium 2017, 2017.

[11] I. Fayyad, Bending cylinders: Ageometric syntax for zero-waste architecture, in: Advances in Architectural Geometry, K. Dörfler et al. (Eds.), pp. 339–354, De Gruyter, 2023 doi:10.1515/9783111162683-026.

[12] L. Scheder-Bieschin, T. Van Mele, P. Block, Curved-crease flat-foldable bending-active plate structures, in: Advances in Architectural Geometry, K. Dörfler et al. (Eds.), pp. 355–368, De Gruyter, 2023. doi: 10.1515/9783111162683-027.

[13] Lamina emergent torsional (LET) joint, Mechanism and Machine Theory 44 (11), pp. 2098–2109, 2009. doi: 10.1016/j.mechmachtheory.2009.05.015.

[14] T. Nelson, R. Lang, N. Pehrson, S. Magleby, L. Howell, Facilitating deployable mechanisms and structures via developable lamina emergent arrays, Journal of Mechanisms and Robotics, 8 031006, 2016. doi:10.1115/1.4031901.

[15] F. Laccone, L. Malomo, J. Perez, N. Pietroni, F. Ponchio, B. Bickel, P. Cignoni, Flexmaps pavilion: a twisted arc made of meso-structured flat flexible panels, in: Proceedings of the IASS Annual Symposium 2019, 2019.

[16] R. J. Lang, L. L. Howell, Laminar emergent flexural fold joints: Planar compliant mechanisms with large-angle near-revolute motion, Extreme Mechanics Letters, 52, 101657, 2022. doi: 10.1016/j.eml.2022.101657.

[17] M. Lee, T. Tachi, Design and evaluation of compliant hinges for deployable thick origami structures, in: Proceedings of the IASS Annual Symposium 2023, 2023.

[18] T. Ohshima, T. Tachi, H. Tanaka, Y. Yamaguchi, Analysis and design of elastic materials formed using 2d repetitive slit pattern, in: Proceedings of the IASS Annual Symposium 2015, 2015.

[19] A. Ghassaei, E. D. Demaine,N. Gershenfeld, Fast, interactive origami simulation using gpu computation, in: Proceedings of the 7th International Meeting on Origami in Science, Mathematics and Education, Vol. 4, Tarquin, Oxford, England, 2018, pp. 1151–1166.

[20] A. Micheletti, I. Giannetti, M. G., A. Tiero, Kinematic and static design of rigid origami structures: Application to modular yoshimura patterns, Journal of Architectural Engineering, 28 (2), 04022009, 2022. doi:10. 1061/(ASCE)AE.1943-5568.000053

[21] A. Micheletti, A. Tiero, G. Tomassetti, Simulation and design of isostatic thick origami structures, Meccanica, 59, 1403–1423, 2024. doi:10.1007/ s11012-024-01815-0.

[22] D. Feshbach, X. Wu, S. Vasireddy, L. Beardell, B. To, Y. Baryshnikov, C. Sung, CurveQuad: a centimeter-scale origami quadruped that leverages curved creases to self-fold and crawl with one motor, 2023 IEEE/RSJ International Conference on Intelligent Robots awwnd Systems (IROS), Detroit, MI, USA, pp. 2485-2492, 2023. doi:10.1109/IROS55552.2023.10342339

[23] Z. Zhai, Y. Wang, K. Lin, L. Wu, H. Jiang, In situ stiffness manipulation using elegant curved origami, Science Advances, 6(47), pp. eabe2000, 2020. doi: 10.1126/sciadv.abe2000